Wang et al. Nanoscale Research Letters (2016) 11:27
DOI 10.1186/s11671-016-1231-1

Nanoscale Research Letters
a SpringerOpen Journal

NANO EXPRESS Open Access

Nitrogen-Doped Carbon Dots for "green" Quantum Dot Solar Cells

Hao Wang[1], Pengfei Sun[1], Shan Cong[1], Jiang Wu[2], Lijun Gao[1*], Yun Wang[1], Xiao Dai[1], Qinghua Yi[1] and Guifu Zou[1*]

Abstract

Considering the environment protection, "green" materials are increasingly explored for photovoltaics. Here, we developed a kind of quantum dots solar cell based on nitrogen-doped carbon dots. The nitrogen-doped carbon dots were prepared by direct pyrolysis of citric acid and ammonia. The nitrogen-doped carbon dots' excitonic absorption depends on the N-doping content in the carbon dots. The N-doping can be readily modified by the mass ratio of reactants. The constructed "green" nitrogen-doped carbon dots solar cell achieves the best power conversion efficiency of 0.79 % under AM 1.5 G one full sun illumination, which is the highest efficiency for carbon dot-based solar cells.

Keywords: Carbon dots, Nitrogen-doped, Quantum dot solar cells

Background

Among the third-generation photovoltaics, quantum dot solar cells (QDSCs) are emerging as a promising candidate due to the unique and versatile characteristics of quantum dots (QDs) including tunable band gap and high absorption coefficient [1–4]. Typically, low-band gap metal chalcogenide (CdS, CdSe, CdTe, PbS, PbSe, $CuInS_2$, etc.) QDs are widely used as sensitizers in QDSCs [5–10]. The QDSCs have been well developed, but they contain highly toxic metals (including Cd, Pb, and In). Hence, the environmentally friendly alternatives ("green" materials) are extremely needed and welcomed to the fabrication of solar cells.

Due to the unique optical and electronic properties, water solubility, excellent biocompatibility, low toxicity, and robust chemical inertness [11–15], carbon dots (CDs) as an emerging carbon-based nanomaterial have been widely researched and applied in many fields [16–22]. One of the CDs applications is tentatively used as sensitizers for QDSCs [23–26]. For instance, Mirtchev et al. [24] have prepared water soluble CDs as sensitizers for QDSCs achieving power conversion efficiency (PCE) of 0.13 %. Zhang et al. [25] have also fabricated 0.13 % PCE of QDSCs based on nitrogen-doped CDs (NCDs). Up to now, the low short-circuit current density (J_{sc}) might be the main factor limiting the efficiency of the cells in comparison with the open-circuit voltage (V_{oc}) and fill factor (FF) of metal chalcogenide-based QDSCs. Narrow light-absorption and diverse trap states result in the extremely low J_{sc} of CD-based QDSCs. Meanwhile, CDs' light-absorption is centered at ultra-violet region and very weak at visible region. Because the existence of trap state defects with different energy levels has been demonstrated by their excitation-dependent fluorescence [27], partially photoinduced carriers will be recombined by CDs rather than being injected into the transporting media. Accordingly, the PCE of QDSCs is very low. Much effort still needs to improve the practicable sensitizers for QDSCs.

In this study, we have developed NCDs to build up the "green" QDSCs with enhanced efficiency. The NCDs were prepared by direct pyrolysis of citric acid and ammonia. Experimental results show that the NCDs' excitonic absorption depends on the N-doping content modified by the mass ratio of reactants. The NCDs with optimal excitonic absorption were used as sensitizers in the QDSCs. The constructed NCD solar cell achieves the best PCE of 0.79 % under AM 1.5 G one full sun illumination. It is noting that the obtained efficiency is the highest one in the reported solar cell-based CDs.

* Correspondence: gaolijun@suda.edu.cn; zouguifu@suda.edu.cn
[1]College of Physics, Optoelectronics and Energy & Collaborative Innovation Center of Suzhou Nano Science and Technology, Soochow University, Suzhou 215006, People's Republic of China
Full list of author information is available at the end of the article

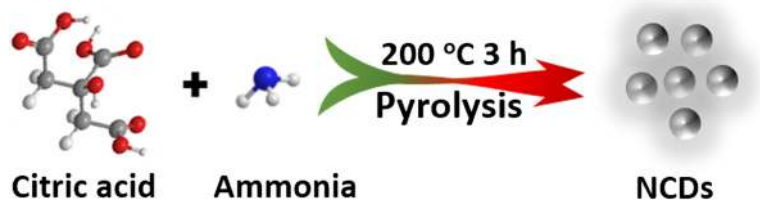

Scheme 1 Preparation of NCDs via direct pyrolysis of citric acid and ammonia

Methods

Synthesis

The NCDs were prepared by a direct pyrolysis method. As shown in Scheme 1, the NCDs are prepared by direct pyrolysis of citric acid (CA, Alfa Aesar) and ammonia (Sinopharm Chemical Reagent Co.) mixture similar to the previous report [28]. Typically, CA (4 g) and certain amount of ammonia are dissolved in distilled water (10 mL) with stirring for 30 min. Then, the prepared solution is transferred into a porcelain boat and then heated in air at 200 °C for 3 h with a heating rate of 10 °C/min. The obtained carbogenic product is mixed with acetone (40 mL, Sinopharm Chemical Reagent Co.) by ultrasonic. The supernatants containing NCDs are collected after centrifugation at 10,000 rpm for 15 min. Then, the acetone is removed by rotary evaporation, and solid-state NCDs are collected for further characterization and usage.

Fabrication of Solar Cell

The NCD-sensitized TiO_2 photoanodes are fabricated according to the previous report [29]. The cleaned fluorine-doped tin oxide (FTO) glasses are immersed in 40 mM $TiCl_4$ aqueous solution at 70 °C for 30 min and washed with water and ethanol. A 20-nm-sized TiO_2 paste is deposited on the FTO glass plate by doctor blade printing technique and then dried at 125 °C for 5 min. The scattering layer of 200-nm-sized TiO_2 paste is coated on the top of the first TiO_2 layer, followed by sintering in air at 500 °C for 30 min. After cooling to 95 °C, the TiO_2 film is immersed in the NCQD acetone solution at room temperature for 2 h. The NCD-sensitized TiO_2 is washed with anhydrous ethanol and dried with nitrogen stream. The solar cells are fabricated by sandwiching gel electrolytes between a NCD-sensitized TiO_2 electrode and a Pt counter electrode, which are separated by a 25-mm-thick hot-melt ring (Surlyn, Dupont) and sealed by heating. The electrolyte injection hole on the thermally platonized FTO counter electrode is finally sealed with Surlyn sheet and a thin glass by heating.

Characterization and Measurement

The morphology of the materials is investigated by transmission electron microscopy (TEM, FEI Tecnai G-20) and atomic force microscopy (AFM, Asylum Research MFP-3D-BIO). Fourier transform infrared (FT-IR) spectra are obtained on a Bruker VERTEX70 FT-IR spectrometer ranged from 4000 to 400 cm^{-1}. X-ray photoelectron spectra (XPS) are acquired with a Japan Kratos Axis Ultra HAS spectrometer using a monochromatic Al Kα source. The crystallinity of NCDs were characterized by Raman spectroscopy (HORIBA Jobin Yvon HR800) using 514-nm laser as the excitation source. The UV–visible absorption spectrum and diffuse-reflectance spectra are recorded on a UV2501PC (Shimadzu). The photoluminescence (PL) spectra are recorded on a Fluoromax-4 spectrofluorometer (HORIBA JobinYvon Inc.) equipped with a 150 W of xenon lamp as the excitation source. Photocurrent–voltage measurements of solar cells (Keithley2440 sourcemeter) are obtained by using a solar simulator (Newport) with an AM 1.5 G filter under an irradiation intensity of 100 $mWcm^{-2}$ (550-W Xe source, Abet). The light intensity is calibrated using a standard silicon photovoltaic solar cell. The active cell area is 0.25 cm^2. All of the measurements above are performed at room temperature.

Results and Discussion

The UV–vis spectra of NCDs from different reactant mass ratios show the NCDs' excitonic absorption strongly depends on their N-doping content (Fig. 1). Our results

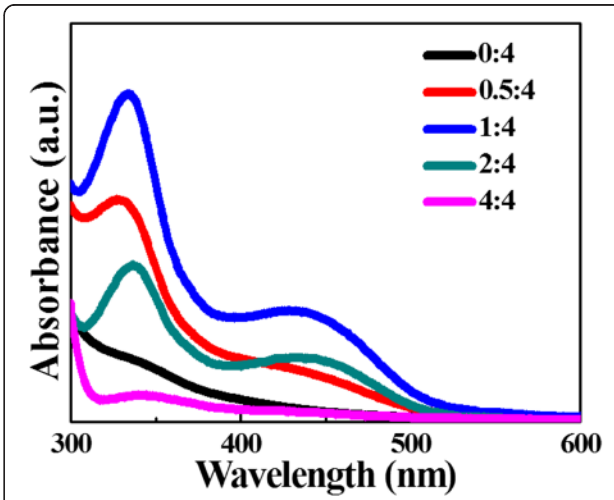

Fig. 1 UV–vis spectra of NCDs from 4 g CA and different amounts (0, 0.5, 1, 2, and 4 g) of ammonia

Table 1 Relative elemental analysis of the CDs with different N-doping levels by XPS analysis

Elemental/atomic (%)	C	O	N
N-free	78.4	21.6	0
0:4	74.8	22.6	2.6
1:4	67.5	22.5	10.0
2:4	69.7	21.1	9.7
4:4	71.5	19.2	9.3

demonstrate that the N-doping content is easily modified by the mass ratio of reactants. When the mass ratio of the reactants ammonia and CA is around 1: 4, the NCDs possess the optimal visible absorption. The excessive ammonia might happen strong chemical reaction with overheated NCDs resulting in excessive amount of water loss and the destruction of NCDs surface. To explore the effect of the mass ratio on the N-doping level of the NCDs, the element constitutes of the NCDs have been analyzed in Table 1. The N-doping content increases with the increasing mass ratio of ammonia and CA. Nevertheless, it changes slight when the mass ratio further increases over 4:1.

The optical properties of optimal NCDs were further studied in Fig. 2. Compared with N-free CDs, the optimal NCDs exhibit not only much higher absorption peak around 335 nm but also more broad absorption band extending to 550 nm (Fig. 2a). In general, the absorption peak around 335 nm corresponds to n–π* transition of C=O bonds while the visible absorption band is attributed to the amino groups on the surface of NCDs [30]. The expanding absorption to 550 nm indirectly explains nitrogen-doping CDs. In addition, NCDs also exhibit excellent solubility with bright blue emission under UV lamp (365 nm) irradiation (inset of Fig. 2a). With the excitation wavelength increasing from 300 to 500 nm in Fig. 2b, the emission intensity gradually decreases and the emission peak shifts from 425 to 510 nm [31]. The surface groups of NCDs introduce trap states with different energy levels resulting in the excitation-dependent emission. The NCDs' fluorescence quantum yield (FLQY) was calculated to be ~36 % with quinine sulfate (FLQY 54 %) as the reference (see Additional file 1: Figure S1).

NCDs were characterized by FT-IR spectroscopy (see Additional file 1: Figure S2). The absorption bands of C–N stretching vibrations at 1182 cm^{-1} confirms the doping of N in the NCDs. Besides, there also observe O–H stretching vibrations at 3000–3400 cm^{-1}, C–H stretching vibrations at 2940 cm^{-1}, C=O stretching vibrations at 1710 cm^{-1}, C–O stretching vibrations at 1408 and 1286 cm^{-1}, C–O–C stretching vibrations at 1350 cm^{-1}. XPS measurements were performed for the surface elemental analysis of NCDs in Fig. 3a. The full-scan spectrum reveals the existence of carbon (C 1 s, 284.5 eV), nitrogen (N 1 s, 400.5 eV), and oxygen (O 1 s, 531.5 eV). In the expanded XPS spectrum (Fig. 3b), carbon's 1-s peaks at 284.6, 285.7, and 288.1 eV can be assigned to bonds of C–C, C–N/C–O, and C=O, respectively. Figure 3c illustrates nitrogen 1-s peaks at 400.3 and 401.6 eV suggesting nitrogen exists in the form of C–N and N–H bonds. As shown in Fig. 3d, oxygen 1-s peak exhibits two peaks at 531.7 and 532.8 eV, which are attributed to C=O and C–OH/C–O–C, respectively. It can be concluded that nitrogen-doped CDs have a variety of polar groups including hydroxyl, alkyl, and carboxyl [32].

The morphology of NCDs was characterized by TEM and AFM in Fig. 4. The TEM images (Fig. 4a, b) show that NCDs' sizes are mainly distributed in the range of 7–15 nm with an average size of 10.8 nm. The AFM image (Fig. 4c–e) depicts that the topographic height of the NCDs is in the range of 1–3 nm with main distribution at 2 nm. It suggests the NCDs have the cylindrical-like structure (similar to small pieces of graphitic layer stacking) [32]. Raman spectroscopy was used to analyze the relative intensity ratio about 1.07 of the D-band (1342 cm^{-1}) and G-band (1531 cm^{-1}) (see Additional file 1: Figure S3).

The enhanced visible-light absorption delivers a message that NCDs could be an attractive interface

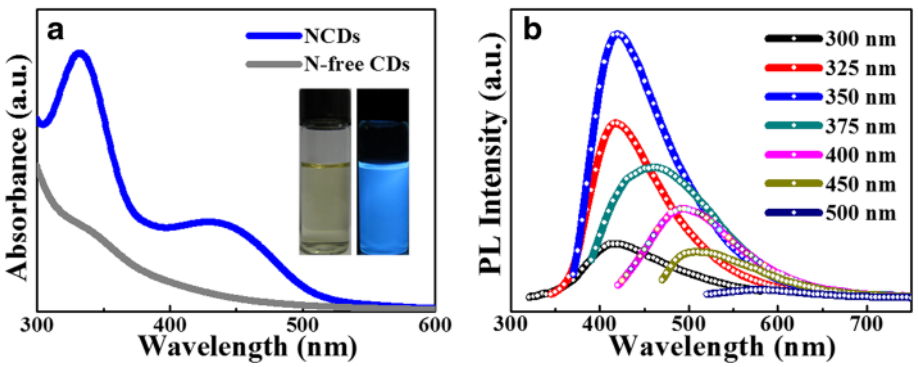

Fig. 2 **a** UV–vis spectra of NCDs and N-free CDs. *Insets* are the photographs of NCDs aqueous solution under day light (*left*) and UV lamp irradiation (*right*). **b** PL spectrum of NCDs with excitation of different wavelengths recorded from 300 to 500 nm

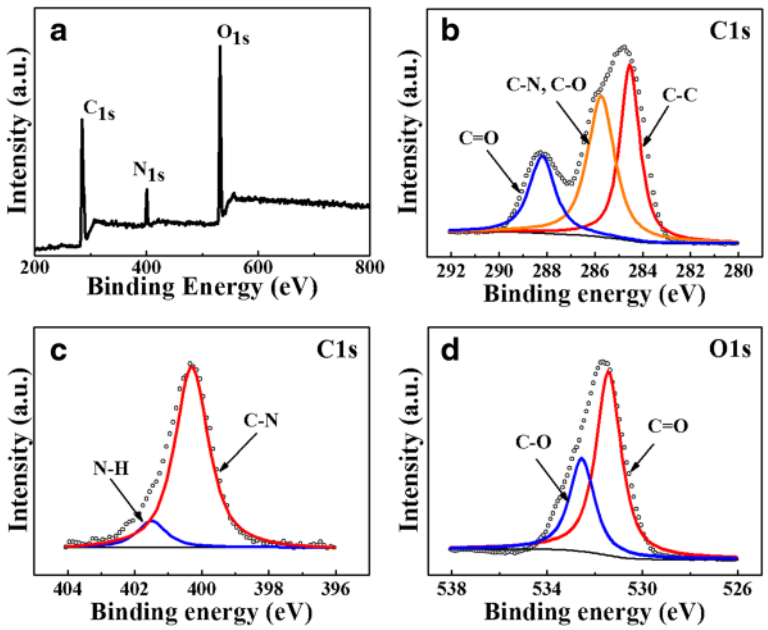

Fig. 3 XPS survey scan of NCDs on indium foil. **a** XPS full scan spectrum. XPS high resolution survey scan of (**b**) C1s, (**c**) N1s, and (**d**) O1s region

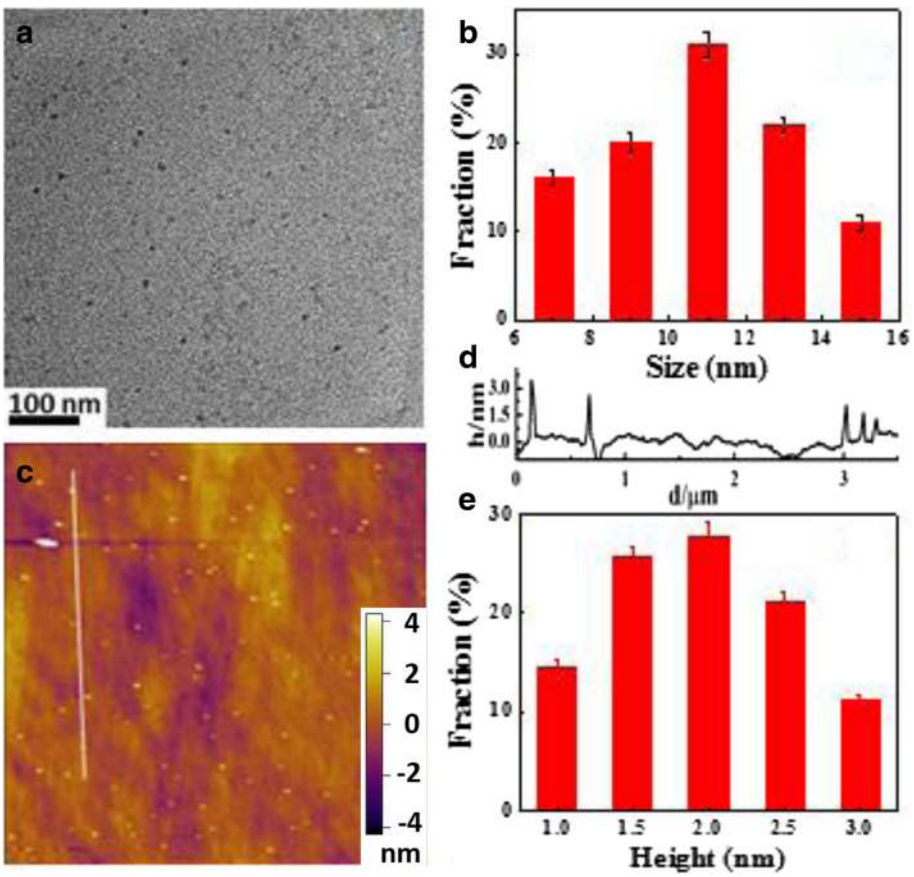

Fig. 4 **a** TEM image of NCDs. **b** Particle size distribution of NCDs. **c** AFM image of NCDs deposited on silicon substrate. **d** Height profile along the white line in (**c**). **e** Height distribution of NCDs

material integrated with porous TiO_2 for QDSCs. As a demonstration, NCQDs were combined with anatase TiO_2. Figure 5a describes UV–vis diffuse reflectance spectrum of TiO_2 (inset: NCDs/TiO_2 photoanode). It could be seen that NCD/TiO_2 photoanode gains much more enhanced absorption in visible region ranging from 400 to550 nm than the pure TiO_2 photoanode. It should be helpful to apply for photosensitizers. Furthermore, the PL spectrum of NCDs, TiO_2, and NCDs/TiO_2 were also studied to confirm the phenomena (see Additional file 1: Figure S4). Under visible light excitation of 420 nm, pure TiO_2 has negligible PL emission while NCDs exhibit a strong and wide emission peak centered at 550 nm. However, it is interesting to see that the emission of NCDs/TiO_2 greatly weakened. It indicates that TiO_2 impedes the recombination of photogenerated electrons and holes in excited NCDs and absorbs the photogenerated electrons. The schematic diagram in Fig. 5b presents the photoinduced electrons transition between NCDs and TiO_2. Compared to N-free CDs, the N-dopant of NCDs can introduce an additional energy level between π of carbon and π* of oxygen. Once excited, NCDs can absorb the relative low-energy photons at visible light range and generate the photoexcited electrons. As a result, there are more electrons transferring to the conducting band of the TiO_2, resulting in the higher current density. To investigate the potential application in photovoltaics, we fabricated NCDs as sensitizers for QDSCs. Figure 5c shows the current density–voltage (J-V) curve of NCDs sensitized solar cells under AM 1.5 G one full sun illumination. The solar cell has a J_{sc} of 2.65 mA cm^{-2}, a V_{oc} of 0.47 V, a FF of 62.5 %, and overall PCE of 0.79 %. To our best knowledge, the PCE is the highest value in the reported QDSCs based on CDs. Incident photon-to-electron conversion efficiency (IPCE) is plotted in Fig. 5d. It was found that the overall photocurrent response closely matches the corresponding absorption spectrum of NCD-sensitized TiO_2 film in Fig. 5a. IPCE value is over 10 % between 400 and 550 nm. It is noting that the highest value of IPCE even approaches 34 % for NCDs.

Conclusions

In summary, we have developed "green" quantum dot solar cells based on nitrogen-doped carbon dots. The optimal NCD-based solar cells achieve a PCE of 0.79 % with J_{sc} of 2.65 mA cm^{-2}, V_{oc} of 0.47 V, and FF of 62.5 %. The obtained PCE is the highest value in the reported QDSCs based on CDs. The study demonstrates that the further optimization of nitrogen dopant can gain a better conversion efficiency of NCD-based solar cells.

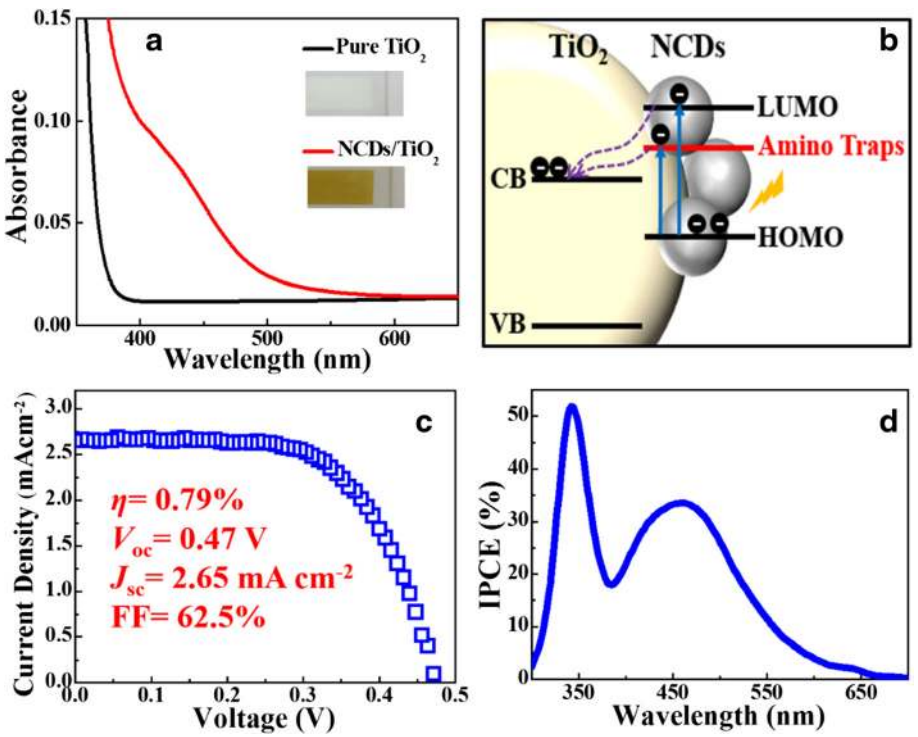

Fig. 5 **a** UV–vis DRS spectra of TiO_2 and NCD/TiO_2 photoanode. *Insets* are the photographs of TiO_2 and NCD/TiO_2 photoanode. **b** A proposed model of photoinduced electron transition between NCDs and TiO_2. **c** Current density–voltage characteristics and (**d**) IPCE action spectrum of NCD-sensitized solar cells

Additional file

Additional file 1: Fluorescence quantum yields and characterizations ofnitrogen-doped carbon dots. (DOCX 87 kb)

Competing Interests
The authors declare that they have no competing interests.

Authors' Contributions
HW carried out all the measurement and drafted the manuscript. PS and SC fabricated the solar cells and analyzed the performance. JW and XD participated in the discussion of the study and helped to write the manuscript. YW carried out the TEM test and QY carried out the AFM test. LG and GZ conceived the study and participated in its design. All authors read and approved the final manuscript.

Acknowledgements
We gratefully acknowledge the support from "973 Program – the National Basic Research Program of China" Special Funds for the Chief Young Scientist (2015CB358600), the Excellent Young Scholar Fund from National Natural Science Foundation of China (21422103), Jiangsu Fund for Distinguished Young Scientist (BK20140010), Jiangsu Specially-Appointed Professor Program (SR10800412), the Priority Academic Program Development of Jiangsu Higher Education Institutions (PAPD), and Jiangsu Scientist and Technological Innovation Team (2013).

Author details
[1]College of Physics, Optoelectronics and Energy & Collaborative Innovation Center of Suzhou Nano Science and Technology, Soochow University, Suzhou 215006, People's Republic of China. [2]Department of Electronic and Electrical Engineering, University College London, Torrington Place, London, UK.

Received: 1 October 2015 Accepted: 5 January 2016
Published online: 19 January 2016

References
1. Semonin E, Luther JM, Choi S, Chen HY, Gao J, Nozik AJ, Beard MC (2011) Peak external photocurrent quantum efficiency exceeding 100 % via MEG in a quantum dot solar cell. Science 334:1530–1533
2. Sargent EH (2012) Colloidal quantum dot solar cells. Nat Photonics 6:133–135
3. Kramer IJ, Sargent EH (2013) The architecture of colloidal quantum dot solar cells: materials to devices. Chem Rev 114:863–882
4. Kim MR, Ma D (2014) Quantum-dot-based solar cells: recent advances, strategies, and challenges. J Phys Chem Lett 6:85–99
5. Santra PK, Kamat PV (2012) Tandem-layered quantum dot solar cells: tuning the photovoltaic response with luminescent ternary cadmium chalcogenides. J Am Chem Soc 135:877–885
6. Zhu H, Song N, Lian T (2013) Charging of quantum dots by sulfide redox electrolytes reduces electron injection efficiency in quantum dot sensitized solar cells. J Am Chem Soc 135:11461–11464
7. Jiao S, Shen Q, Mora-Seró I, Wang J, Pan Z, Zhao K, Kuga Y, Zhong X, Bisquert J (2015) Band engineering in core/shell ZnTe/CdSe for photovoltage and efficiency enhancement in exciplex quantum dot sensitized solar cells. ACS Nano 9:908–915
8. Zhang J, Gao J, Church CP, Miller EM, Luther JM, Klimov VI, Beard MC (2014) PbSe quantum dot solar cells with more than 6 % efficiency fabricated in ambient atmosphere. Nano Lett 14:6010–6015
9. Speirs MJ, Balazs DM, Fang HH, Lai LH, Protesescu L, Kovalenko MV, Loi MA (2015) Origin of the increased open circuit voltage in PbS-CdS core-shell quantum dot solar cells. J Mater Chem A 3:1450–1457
10. Pan Z, Mora-Seró I, Shen Q, Zhang H, Li Y, Zhao K, Wang J, Zhong X, Bisquert J (2014) High-efficiency "green" quantum dot solar cells. J Am Chem Soc 136:9203–9210
11. Lim SY, Shen W, Gao Z (2015) Carbon quantum dots and their applications. Chem Soc Rev 44:362–381
12. Ge J, Lan M, Zhou B, Liu W, Guo L, Wang H, Jia Q, Niu G, Huang X, Zhou H, Meng X, Wang P, Lee CS, Zhang W, Han X (2014) A graphene quantum dot photodynamic therapy agent with high singlet oxygen generation. Nat Commun 5:4596
13. Baker SN, Baker GA (2010) Luminescent carbon nanodots: emergent nanolights. Angew Chem Int Ed 49:6726–6744
14. Liu RL, Wu DQ, Liu SH, Koynov K, Knoll W, Li Q (2009) An aqueous route to multicolor photoluminescent carbon dots using silica spheres as carriers. Angew Chem Int Ed 48:4598–4601
15. Zhao QL, Zhang ZL, Huang BH, Peng J, Zhang M, Pang DW (2008) Facile preparation of low cytotoxicity fluorescent carbon nanocrystals by electrooxidation of graphite. Chem Commun 41:5116–5118. doi:10.1039/b812420e
16. Wang L, Wang Y, Xu T, Liao H, Yao C, Liu Y, Li Z, Chen Z, Pan D, Sun L, Wu M (2014) Gram-scale synthesis of single-crystalline graphene quantum dots with superior optical properties. Nat Commun 5:5357
17. Ding C, Zhu A, Tian Y (2014) Functional surface engineering of C-dots for fluorescent biosensing and in vivo bioimaging. Acc Chem Res 47:20–30
18. Zhu Z, Ma J, Wang Z, Mu C, Fan Z, Du L, Bai Y, Fan L, Yan H, Phillips DL (2014) Efficient enhancement of perovskite solar cells through fast electron extraction: the role of graphene quantum dots. J Am Chem Soc 136:3760–3763
19. Wang H, Gao P, Wang Y, Guo J, Zhang KQ, Du D, Dai X, Zou G (2015) Fluorescently tuned nitrogen-doped carbon dots from carbon source with different content of carboxyl groups. APL Mater 3:086102
20. Wang H, Wang Y, Guo J, Su Y, Sun C, Zhao J, Luo H, Dai X, Zou G (2015) A new chemosensor for Ga^{3+} detection by fluorescent nitrogen-doped graphitic carbon dots. RSC Adv 5:13036–13041
21. Li H, He X, Kang Z, Huang H, Liu Y, Liu J, Lian S, Tsang CHA, Yang X, Lee ST (2010) Water-soluble fluorescent carbon quantum dots and photocatalyst design. Angew Chem Int Ed 49:4430–4434
22. Mao LH, Tang WQ, Deng ZY, Liu SS, Wang CF, Chen S (2014) Facile access to white fluorescent carbon dots toward light-emitting devices. Ind Eng Chem Res 53:6417–6425
23. Yan X, Cui X, Li B, Li LS (2010) Large, solution-processable graphene quantum dots as light absorbers for photovoltaics. Nano Lett 10:1869–1873
24. Mirtchev P, Henderson EJ, Soheilnia N, Yip CM, Ozin GA (2012) Solution phase synthesis of carbon quantum dots as sensitizers for nanocrystalline TiO_2 solar cells. J Mater Chem 22:1265–1269
25. Zhang YQ, Ma DK, Zhang YG, Chen W, Huang SM (2013) N-doped carbon quantum dots for TiO_2-based photocatalysts and dye-sensitized solar cells. Nano Energy 2:545–552
26. Sun M, Ma X, Chen X, Sun Y, Cui X, Lin Y (2014) A nanocomposite of carbon quantum dots and TiO_2 nanotube arrays: enhancing photoelectrochemical and photocatalytic properties. RSC Adv 4:1120–1127
27. Li X, Zhang S, Kulinich SA, Liu Y, Zeng H (2014) Engineering surface states of carbon dots to achieve controllable luminescence for solid-luminescnet composites and sensitive Be^{2+} detection. Sci Rep 4:4976
28. Dong Y, Shao J, Chen C, Li H, Wang R, Chi Y, Lin X, Chen G (2012) Blue luminescent graphene quantum dots and graphene qxide prepared by tuning the carbonization degree of citric acid. Carbon 50:4738–4743
29. Li Q, Zhao J, Sun B, Lin B, Qiu L, Zhang Y, Chen X, Lu J, Yan F (2012) High-temperature solid-state dye-sensitized solar cells based on organic ionic plastic crystal electrolytes. Adv Mater 24:945–950
30. Zhang X, Zhang Y, Wang Y, Kalytchuk S, Kershaw SV, Wang Y, Wang P, Zhang T, Zhao Y, Zhang H, Cui T, Wang Y, Zhao J, Yu WW, Rogach AL (2013) Color-switchable electroluminescence of carbon dot light-emitting diodes. ACS Nano 7:11234–11241
31. Wu ZL, Zhang P, Gao MX, Liu CF, Wang W, Leng F, Huang CZ (2013) One-pot hydrothermal synthesis of highly luminescent nitrogen-doped amphoteric carbon dots for bioimaging from Bombyx mori silk-natural proteins. J Mater Chem B 1:2868–2873
32. Li Y, Zhao Y, Cheng H, Hu Y, Shi G, Dai L, Qu L (2011) Nitrogen-doped graphene quantum dots with oxygen-rich functional groups. J Am Chem Soc 134:15–18